

RSC Advances

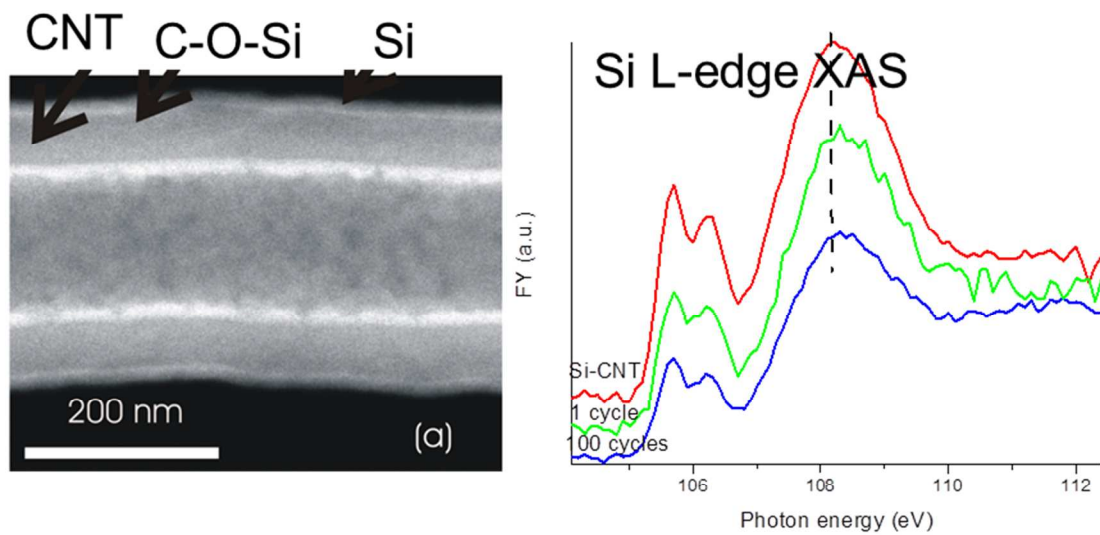


This is an *Accepted Manuscript*, which has been through the Royal Society of Chemistry peer review process and has been accepted for publication.

Accepted Manuscripts are published online shortly after acceptance, before technical editing, formatting and proof reading. Using this free service, authors can make their results available to the community, in citable form, before we publish the edited article. This *Accepted Manuscript* will be replaced by the edited, formatted and paginated article as soon as this is available.

You can find more information about *Accepted Manuscripts* in the [Information for Authors](#).

Please note that technical editing may introduce minor changes to the text and/or graphics, which may alter content. The journal's standard [Terms & Conditions](#) and the [Ethical guidelines](#) still apply. In no event shall the Royal Society of Chemistry be held responsible for any errors or omissions in this *Accepted Manuscript* or any consequences arising from the use of any information it contains.



The Si-O-C bonding and its evolution upon electrochemical cycling in Si coated-carbon nanotube anode are unveiled by X-ray absorption spectroscopy studies.

COMMUNICATION

Chemical bonding in amorphous Si coated-carbon nanotube as anode for Li ion battery: a XANES study

Cite this: DOI: 10.1039/x0xx00000x

Jigang Zhou^{a,c*}, Yongfeng Hu^a, Xiaolin Li^b, Chongmin Wang^{b*}, and Lucia Zuin^a

Received 00th January 2012,
Accepted 00th January 2012

DOI: 10.1039/x0xx00000x

www.rsc.org/

The chemical bonding nature and its evolution upon electrochemical cycling in amorphous Si coated-carbon nanotube (Si-CNT) anode has been investigated using comprehensive X-ray absorption spectroscopy (XANES) at Si L- and K-edges along with C and O K-edges. The Si nanolayer on CNT is found to be anchored to CNT via Si-O-C bonding. This bond weakens upon electrochemical cycling accompanied with generation of Li_2CO_3 on the surface of Si-CNT. Those findings are crucial in designing further improved Si-C composite anode for lithium ion battery.

Nanostructured Si, especially when hybridized with carbon, offers a plausible solution to utilize the high theoretical capacity of Si but without concerns of the structural damage due to the extremely large volume change (300%) during the lithiation/delithiation cycle^{1, 2}. Given that the Si-C composite relies on the electronic conductivity of carbon, the interaction of Si with carbon and its maintenance during electrochemical lithiation/delithiation cycling are crucial for a high performance lithium ion battery anode. In-situ TEM investigation has been applied to study phase transformation and microstructural evolution of amorphous silicon nano-layer coated carbon nanotube (Si-CNT), which finds that the Si layer is strongly bonded to CNT and no spallation during lithiation and delithiation cycles². However a deeper and fundamental understanding of the electronic nature of bonding between Si layer and CNT in Si-CNT and its evolution upon cycling is still needed to provide insights of the structural stability in Si-CNT as the anode and its failing mechanism. This information will not only benefit Si-CNT study but will serve as a model for other Si-C³ based lithium ion battery anodes to lead further performance improvements. In addition to the Si-C interaction in Si-CNT, study of the solid-electrolyte interface (SEI), a layer of decomposed electrolyte upon cycling on the surface in this Si-CNT anode is also needed for further understanding of its stable cycling performance. Relevantly, Si oxidation state change upon lithiation shall unveil the charge compensation mechanism

during lithiation⁴, which is important to a full understanding of the lithiation process. X-ray absorption near edge structure (XANES) spectroscopy involves the measurement and interpretation of the photoabsorption cross-section across a particular core level (absorption edge) of an atom in a chemical environment up to ~50 eV above the threshold. The absorption features in XANES track bound to bound and bound to quasi-bound (multiple scattering) transitions thus affording element specificity and they are very sensitive to the local chemical environment of the absorbing atom. XANES has been applied successfully to reveal the fundamental structure and bonding in nanomaterial, particularly carbon nanostructure hybrid⁵⁻⁷, and also chemical interaction in graphene based lithium ion battery electrode materials^{4, 8}. O K-edge XANES is known to be very sensitive to various Li oxide and carbonate compounds⁹ which are the major components of a SEI layer¹⁰. This letter reports an application of C, O, Si K-edges and Si L-edge XANES to study the chemical nature of the Si-C interaction and its evolution along cycling in Si-CNT. Along this main goal, the SEI and Si oxidation state and their change upon cycling will also be studied. Such goals can only be achieved with a comprehensive X-ray spectroscopic study by probing different elements and/or different edges of the same element in a complex system. The former allows a full perspective view of a bonding environment involving of different elements while the latter can access the different orbitals for the same element.

Si-CNT was prepared by chemical vapor deposition of a thin layer Si (~ 13 nm) onto CNTs with a diameter of 100-200 nm (Figure S1a in the support information). CNT before Si coating has amorphous surface which could be served as a link layer to anchor the coated Si as being seen in Figure S1a. TEM and EDX mapping also clarifies the uniform Si coating (Figure S1d and S1e in the support information). The silicon to carbon ratio is 1:3 and the specific capacity of ~ 1000mAh/g of Si-CNT (Figure S1f

in the support) was determined in a coin cell which consisted of Si-CNT electrode and Li metal counter electrode with EC/DEC as the electrolyte². The coin cell was cycled at the current rate of 1A/g with the cut-off voltage at 0.05V for lithiation and 1.5V for the delithiation. The XANES experiment of pristine and cycled Si-CNTs was performed at SGM and PGM beamline in a vacuum chamber at $\sim 10^{-8}$ torr and data was recorded in the surface sensitive total electron yield (TEY, sensitive to the top ~ 5 nm) and bulk sensitive fluorescence yield (FY). For the cycled samples, coin cell was disassembled in a glove box which is attached to the beamline, and loaded directly into the vacuum chamber. XANES data were first normalized to the incident photon flux I_0 measured with a fresh gold mesh at SGM and a Ni mesh at PGM located upstream of the sample. After background correction, the XANES was normalized to the edge jump (the difference in absorption coefficient just below and at a flat region above the edge).

The Si-C interaction in Si-CNT is first explored by comparing C K-edge XANES between CNT and Si-CNT as shown in Fig. 1a. C K-edge XANES reflects the transition from C 1s electrons to mainly C 2p states following the dipole selection rules. It is featured by two main transitions at ~ 285 and ~ 292 eV attributable to C 1s transition to the graphitic C-C (sp^2 carbon) π^* and C-C σ^* state, respectively, in CNT and its composite. The observation of C-C π^* and C-C σ^* in Si-CNT confirms the existence of the graphitic network after Si coating. Along with those two features, a broad peak centered at ~ 288 eV presents in both samples. This peak has been observed in various carbon nanostructures and can be attributed to C-O bond^{6, 8, 11, 12}. It is also well accepted that this feature will be enhanced whenever the carbon nanostructure is hybridized with another components including metal oxide and phosphate which then has been identified as a reliable spectroscopic indicator of the covalent bonding in those nano-hybrids¹²⁻¹⁴. Apparently, this absorption feature is greatly enhanced in Si-CNT relative to that in pristine CNT and this is the first solid spectroscopic evidence of covalent bonding between Si and CNT in Si-CNT, quite possibly in the form of Si-O-C. Such bonding also alters the electronic structure in C 2p orbitals in Si-CNT as seen of the negative energy shift and decreased intensity of the C-C π^* peak. This could suggest a even better electronic conductivity in Si-CNT due to the increase of the electrons closer to the conduction band, which might be comparable to the situation in the conductive polymer binder in high capacity battery anode¹⁵. The proposed Si-O-C bonding can be further evaluated by O K-edge XANES of Si-CNT and CNT which are shown in Fig. 1b. O K-edge probes the unoccupied O 2p projected states which could be hybridized with carbon or silicone states. CNT presents a broad peak at ~ 532 eV which can be due to the π^* of the C-O bond¹⁶. The observation of this peak, together with the assignment of ~ 288 eV peak in C K-edge in Fig. 1a, confirm the existence of oxygen functional groups in pristine CNT. This C-O bonding has an associated σ^* bonding feature at ~ 540 eV which is also called shape resonance peak due to its intrinsic sensitivity to the bond length similar to the case in the N K-edge XANES study of C-N bond¹⁷. Interestingly, upon Si coating this shape resonance peak shifts to lower energy which means a loose bonded O relative to that in pristine CNT. This agrees well with the fact that Si has larger atomic radius and

weaker electron affinity compared to carbon, thus a Si-O bond is expected to have a weaker covalent feature than in a C-O bond. Therefore this is the second spectroscopic evidence of the formation of Si-O-C bond in the interface between Si and CNT in Si-CNT. Si takes sp^3 hybridization to bond with oxygen therefore the Si-O-C bond results in lower intensity of π^* at ~ 532 eV.

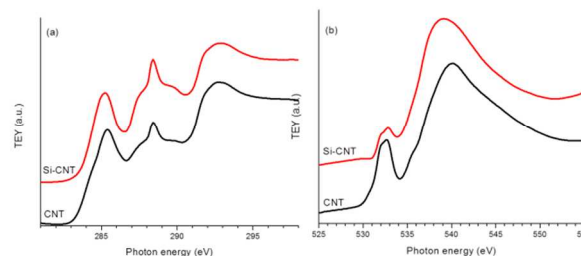


Fig.1 TEY C K-edge XANES (a) and O K-edge XANES (b) of CNT and Si-CNT.

We will focus next on the C and O K-edge XANES of lithiated Si-CNTs to explore the Si-O-C bond change upon electrochemical lithiation and cycling of lithiation/delithiation before we use Si L and K-edge XANES to explore this Si-O-C bonding and its evolution. Upon lithiation, a passivating SEI layer with Li_2CO_3 as the majority¹⁸ was expected to form on Si-CNT which blocks TEY signal from CNT from being detected, resulting in a much lower C-C π^* in lithiated Si-CNT relative to that in pristine Si-CNT (see Fig S.2 for the C K-edge TEY spectra in the support information). To probe the Si-O-C bond in the SEI coated Si-CNT, bulk sensitive FY mode was used to collect C K-edge XANES of lithiated Si-CNT along with the pristine Si-CNT and the spectra are displayed in Fig. 2a. Apparently lithiation dramatically sharpens the Si-O-C bond peak (288 eV) which could be due to the strain caused by the large volume expansion in the lithiated Si layer. The intensity of this feature decreases further after 100 cycles of lithiation/delithiation which is highly likely related to a weaker Si-O-C bond in the cycled samples. The weaker Si-O-C bond can also be reflected by the O K-edge XANES as displayed in Fig. 2b. As being discussed above in Fig. 1b, the shape resonance peak at around 540 eV can be used to understand the Si-O-C bonding in Si-CNT. It can be observed that lithiation broadens this peak and cycling shifts this peak to a higher energy, similar to that of pristine Si-CNT. This aligns well with the decrease in the intensity of the 288 eV peak in C K-edge XANES as Si-O-C bond becomes weaker upon lithiation and electrochemical cycling. Along with this observation, the sharp peak at ~ 290 eV at C K-edge and at ~ 535 eV at O K-edge XANES of lithiated Si-CNT indicates the presence of Li_2CO_3 ¹⁹ in SEI. It should be noted that the SEI is very complex and contains other Li species, such as LiO_x which could be identified by O K-edge XANES¹⁹. The spectroscopic difference between lithiated Si-CNTs (cycle 1 and cycle 100) should also be caused by the SEI difference. For instance, there might be more Li_2CO_3 in Si-CNT with 100 cycles and there might be more LiO_x in Si-CNT with only one cycle as shown by the broadened feature close to 535 eV¹⁹.

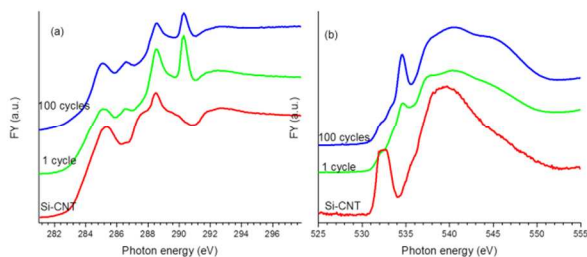


Fig.2 XANES of Si-CNT and lithiated Si-CNTs at C K-edge recorded in FY mode (a), and O K-edge (b) recorded at FY mode.

The Si-O-C bonding in Si-CNT and its evolution is further explored from Si perspective with the Si L-edge XANES displayed in Fig. 3. Si L-edge XANES involves electronic transition of Si 2p states and it is also sensitive to the oxidation state. Again, due to the shallow probing depth at TEY mode ($\sim 5\text{nm}$) only bulk sensitive FY is possible to explore the Si-O-C interface in Si-CNT and lithiated Si-CNT. TEY mode Si L-edge XANES of Si-CNT shows elemental Si feature at $\sim 100\text{ eV}$ but no Si-O feature detectable (Support information Fig. S3) which strengthens the buried interface nature of Si-O-C bond in Si-CNT. Elemental and lithiated Si are present in FY mode Si L-edge XANES but we will only focus Si-O region in Fig.3, as the FY Si L-edge suffers from the self-absorption with partially inverted features²⁰ (Support information Fig. S4). The first two well resolved peaks are transitions to the first unoccupied 3s like states from the spin-orbit split Si 2p ($2p_{3/2}$ and $2p_{1/2}$). Peak at $\sim 108\text{ eV}$ is owing to 2p to 3d transition which features a broad peak (due to multiple scattering). It is generally agreed the splitting and relative peak ratio of first two peaks relates to the long range order of Si-O tetrahedral coordination: the splitting of the peaks becomes more resolved and the peak ratio of first/second peak increases with the increase of the shared oxygen atoms²¹. Clearly, lithiation and further cycling reduces the peak splitting and also the peak ratio of first/second peak which indicates a more amorphous Si-O bond. This must be closely related to a weaker Si-O-C bond in lithiated and cycled Si-CNT. Along with the change of the first two peaks the broad peak at 108 eV also slightly shifts to higher energy upon lithiation which could be linked to a compressed Si-O bond caused by the strain effect due the volume change in Si.

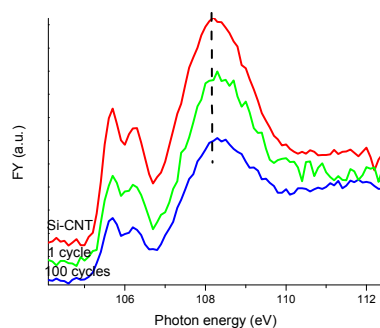


Fig.3 Si L-edge XANES of Si-CNT and lithiated Si-CNT recorded in FY mode.

Finally, the chemical state of Si and Li in lithiated Si-CNT was examined by Si K-edge XANES (TEY) to glean an insight of the lithiation process as being shown in Fig. 4. The Si K-edge arises from the transition of excitations of Si 1s electron to the unoccupied orbitals with p character dominated. It is very sensitive to the Si oxidation state such as that SiO_2 has a characteristic peak at $\sim 1850\text{ eV}$ and Si shows up at $\sim 1845\text{ eV}$ ²². With this as the guide it is clear that the oxidation state in Si-CNT is close to elemental Si with detectable Si-O feature as being observed in Si L-edge and C and O K-edge in above section. Lithiation shifts the absorption edge to lower energy which indicates the oxidation state of Si goes to negative. It makes sense with the consideration of the low electron affinity of Li relative to that of Si thus a charge transfer from Li to Si is expected resulting in a negative covalence for Si in SiLi alloy. In addition to the negative edge shift, a new feature at $\sim 1848\text{ eV}$ shows upon lithiation. This might be also due to the lithiation but we could not exclude the possibility of a distorted Si-O in the Si-C interface or contribution from SEI. Further cycling moves the Si K-edge absorption back to higher energy though the oxidation state shall still be negative. Such spectroscopic difference between lithiated Si-CNT with different cycles clarifies their chemical difference which could be used to explore the electrode fading mechanism.

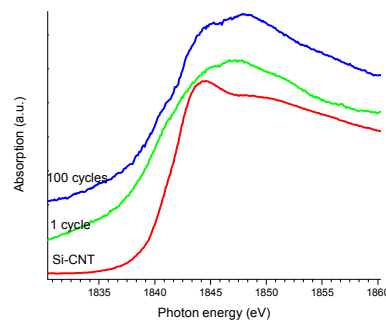


Fig.4 Si K-edge XANES of Si-CNT and lithiated Si-CNT (1 cycle and 100 cycles).

In summary, the detailed chemical interaction nature at the Si-C interface in Si-CNT structure have been studied by comprehensive XANES involving multiple elements and edges. The most possible interaction which anchors the Si layer onto CNT is found to be the Si-O-C bond. This bond was distorted upon lithiation and repeated cycling which becomes more amorphous. Such observation agrees with our previous publication that repeated cycling changes the morphology of Si coating² and also matches the TEM results in the support information (Fig. S1. b and c). Lithiation also generates a passivating layer which consists of Li_2CO_3 . Finally, the charge goes to Si site upon lithiation as being examined by the Si K-edge. These observations shall be useful for further development of better Si-C based Si composite anode, especially when theoretical

calculation and modelling are combined to fully understand the Si-O-C bonding nature and its behaviour in the lithiation.

Notes and references

Thank Drs. J. Dynes and T. Regier at CLS for technical assistances. CLS is supported by NSERC, NRC, CIHR and the University of Saskatchewan. We thank Dr. D. J. Burton of Applied Science for providing the Si-CNT sample. CW thank the support of Chemical Imaging Initiative of Pacific Northwest National Laboratory. Part of the work was conducted in the William R. Wiley Environmental Molecular Sciences Laboratory (EMSL), a national scientific user facility sponsored by DOE's Office of Biological and Environmental Research and located at PNNL. PNNL is operated by Battelle for the Department of Energy under Contract DE-AC05-76RLO1830.

^a Canadian Light Source Inc, Saskatoon, Canada. Fax: 1-306-6573535; Tel: 1-306-657-3587; E-mail: jigang.zhou@lightsource.ca

^b Pacific Northwest National Laboratory, Richland, Washington, 99354, USA; Chongmin.wang@pnnl.gov

^c School of chemical engineering, Harbin Institute of Technology, China

† Footnotes should appear here. These might include comments relevant to but not central to the matter under discussion, limited experimental and spectral data, and crystallographic data.

Electronic Supplementary Information (ESI) available: [TEM and EDS of Si-CNT and lithiated Si-CNT, electrochemical performance, C K-edge of lithiated Si-CNT at TEY mode and Si L-edge XANES at FY mode.]. See DOI: 10.1039/c000000x/

- L. Hu, H. Wu, Y. Gao, A. Cao, H. Li, J. McDough, X. Xie, M. Zhou and Y. Cui, *Adv. Energy Mater.*, 2011, **1**, 523.
- C.-M. Wang, X. Li, Z. Wang, W. Xu, J. Liu, F. Gao, L. Kovarik, J.-G. Zhang, J. Howe, D. J. Burton, Z. Liu, X. Xiao, S. Thevuthasan and D. R. Baer, *Nano Lett*, 2012, **12**, 1624-1632.
- A. Magasinski, P. Dixon, B. Hertzberg, A. Kvit, J. Ayala and G. Yushin, *Nat. Mater.*, 2010, **9**, 353.
- J. G. Zhou, J. Wang, Y. F. Hu, T. Regier, H. L. Wang, Y. Yang, Y. Cui and H. J. Dai, *Chem Commun*, 2013, **49**, 1765-1767.
- J. G. Zhou, H. T. Fang, Y. F. Hu, T. K. Sham, C. X. Wu, M. Liu and F. Li, *J. Phys. Chem. C*, 2009, **113**, 10747-10750.
- J. G. Zhou, H. T. Fang, J. M. Maley, J. Y. P. Ko, M. Murphy, Y. Chu, R. Sammynaiken and T. K. Sham, *J. Phys. Chem. C*, 2009, **113**, 6114-6117.
- S. Yang, D. Wang, G. Liang, Y. M. Yiu, J. Wang, L. Liu, X. Sun and T.-K. Sham, *Energy & Environmental Science*, 2012.
- J. G. Zhou, J. Wang, L. Zuin, T. Regier, Y. F. Hu, H. L. Wang, Y. Y. Liang, J. Maley, R. Sammynaiken and H. J. Dai, *Phys. Chem. Chem. Phys.*, 2012, **14**, 9578-9581.
- B. M. Gallant, D. G. Kwabi, R. R. Mitchell, J. Zhou, C. V. Thompson and Y. Shao-Horn, *Energy & Environmental Science*, 2013, **6**, 2518-2528.
- S. Chattopadhyay, A. L. Lipson, H. J. Karmel, J. D. Emery, T. T. Fister, P. A. Fenter, M. C. Hersam and M. J. Bedzyk, *Chem. Mater.*, 2012, **24**, 3038-3043.
- J. G. Zhou, J. Wang, H. T. Fang, C. X. Wu, J. N. Cutler and T. K. Sham, *Chem. Commun.*, 2010, **46**, 2778-2780.
- Y. Y. Liang, Y. G. Li, H. L. Wang, J. G. Zhou, J. Wang, T. Regier and H. J. Dai, *Nat. Mater.*, 2011, **10**, 780-786.
- Y. Y. Liang, H. L. Wang, P. Diao, W. Chang, G. S. Hong, Y. G. Li, M. Gong, L. M. Xie, J. G. Zhou, J. Wang, T. Z. Regier, F. Wei and H. J. Dai, *J. Am. Chem. Soc.*, 2012, **134**, 15849-15857.
- Y. Y. Liang, H. L. Wang, J. G. Zhou, Y. G. Li, J. Wang, T. Regier and H. J. Dai, *J. Am. Chem. Soc.*, **134**, 3517-3523.
- M. Wu, X. Xiao, N. Vukmirovic, S. Xun, P. K. Das, X. Song, P. Olalde-Velasco, D. Wang, A. Z. Weber, L.-W. Wang, V. S. Battaglia, W. Yang and G. Liu, *J. Am. Chem. Soc.*, 2013, **135**, 12048-12056.
- D. W. Lee, L. De Los Santos V, J. W. Seo, L. L. Felix, A. Bustamante D, J. M. Cole and C. H. W. Barnes, *J. Phys. Chem. B*, 2010, **114**, 5723-5728.
- J. G. Zhou, X. T. Zhou, R. Y. Li, X. L. Sun, Z. F. Ding, J. Cutler and T. K. Sham, *Chem. Phys. Lett.*, 2009, **474**, 320-324.
- M. Nie, D. P. Abraham, Y. Chen, A. Bose and B. L. Lucht, *J. Phys. Chem. C*, 2013, **117**, 13403-13412.
- B. M. Gallant, R. R. Mitchell, D. G. Kwabi, J. G. Zhou, L. Zuin, C. V. Thompson and Y. Shao-Horn, *J. Phys. Chem. C*, 2012, **116**, 20800-20805.
- Y. F. Hu, R. Boukherroub and T. K. Sham, *J. Electron Spectrosc. Relat. Phenom*, 2004, **135**, 143-147.
- S. A. Shaw, D. Peak and M. J. Hendry, *Geochimica et Cosmochimica Acta*, 2009, **73**, 4151-4165.
- Y. F. Hu, H. Piao, J. Fronheiser and K. Matocha, *J. Electron Spectrosc. Relat. Phenom*, 2011, **184**, 245-248.